

FIBER-OPTIC SOURCES OF QUANTUM ENTANGLEMENT

PREM KUMAR, XIAOYING LI, MARCO FIORENTINO, PAUL L. VOSS,
JAY E. SHARPING, AND GERALDO A. BARBOSA

*Center for Photonic Communication and Computing, ECE Department
Northwestern University, 2145 N. Sheridan Road, Evanston, IL 60208-3118
E-mail: kumarp@northwestern.edu*

We present a fiber-based source of polarization-entangled photon pairs that is well suited for quantum communication applications in the $1.5\mu\text{m}$ band of standard telecommunication fiber. Quantum-correlated signal and idler photon pairs are produced when a nonlinear-fiber Sagnac interferometer is pumped in the anomalous-dispersion region of the fiber. Recently, we have demonstrated nonclassical properties of such photon pairs by using Geiger-mode InGaAs/InP avalanche photodiodes. Polarization entanglement in the photon pairs can be created by pumping the Sagnac interferometer with two orthogonally polarized pulses. In this case the parametrically scattered signal-idler photons yield biphoton interference with $> 90\%$ visibility in coincidence detection, while no interference is observed in direct detection of either the signal or the idler photons.

1 Introduction

Quantum entanglement refers to the nonclassical dependency of physically separable quantum systems. It is an essential resource that must be freely available for implementing many of the novel functions of quantum information processing, such as database searching, clock synchronization, teleportation, computing, and cryptography.¹ Therefore, the efficient generation and transmission of quantum entanglement is of prime importance. With the ubiquitous standard optical fiber serving as the transmission medium and the widespread availability of efficient active and passive fiber devices, technological synergy between the generation and propagation components of the overall quantum network can be achieved by deploying sources of entanglement that rely on the nonlinearity of the fiber itself. In order to develop such sources, we have been conducting experiments with fiber-optic devices that can be used as building blocks for fiber-based sources of either polarization or quadrature entanglement. In the polarization case, our fiber-based setup for single-photon quantum optics has the advantage of modal purity over its crystal counterparts,^{2,3} which would be very important for realizing complex networks involving several nonlinear elements.

2 An All-Fiber Source of Quantum-Correlated Photon Pairs

In our effort to develop fiber-based sources of entanglement, we have been investigating nondegenerate four-wave mixing in standard dispersion-shifted fiber (DSF), wherein two pump photons scatter through the Kerr nonlinearity of the fiber to create simultaneous signal and idler photons. Our experiment

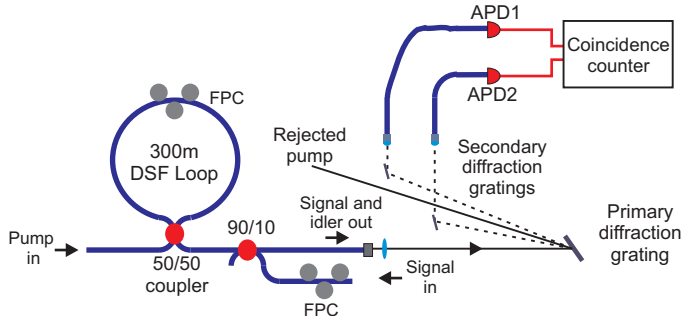


Figure 1. Schematic of the experimental setup. Dispersion-shifted-fiber (DSF) loop and the 50/50 coupler constitute the NFSI. FPC, fiber polarization controller; APD, avalanche photodiode. The signal-in port is blocked during photon-counting measurements.

is conducted near the zero-dispersion wavelength of the DSF, where such scattering is enhanced owing to phase matching of the photon wave functions. It must be pointed out here that in a conventional wavelength-division-multiplexed classical optical communication line, one strives to suppress the four-wave or four-photon mixing process, which otherwise causes cross-talk between the wavelength channels and sets limits on the total data capacity of the communication line.

As shown in Fig. 1, the four-photon mixing takes place in a nonlinear-fiber Sagnac interferometer (NFSI), which we have previously used to generate quantum-correlated twin beams in the fiber.⁴ The pump is a mode-locked train of $\simeq 3$ ps long pulses that arrive at a 75.3 MHz repetition rate. The pulsed operation serves two important purposes: i) the NFSI amplifier can be operated at low average powers and ii) the production of the fluorescence photons is confined to well-defined temporal windows, allowing a gated detection scheme to be used to increase the signal-to-noise ratio. To measure the non-classical (i.e., quantum) correlations between the signal and the idler photons, one must effectively suppress the pump photons from reaching the detectors. Since a typical pump pulse contains $\simeq 10^8$ photons and we are interested in detecting $\simeq 0.01$ signal/idler photon pairs per pulse, a pump-to-signal (idler) rejection ratio in excess of 100 dB is required. We achieve this specification by sending the fluorescence photons through a free-space double-grating spectral filter that separates the signal and idler photons from each other and from the pump photons not rejected by the NFSI (see Fig. 1).

To demonstrate the quantum nature of such four-photon scattering at the “single” photon level, we have assembled a photon-counting apparatus for detecting the signal and idler photons in coincidence. This apparatus is based on commercial InGaAs avalanche photodiodes operating in the gated Geiger mode. Use of this apparatus has allowed us to verify the simultaneous production of the signal and idler photon pairs.⁵ In the inset in Fig. 2 we show the number of scattered photons, N_I (N_S), detected in the idler (signal) channel as a function of the number of pump photons, N_P , injected into the

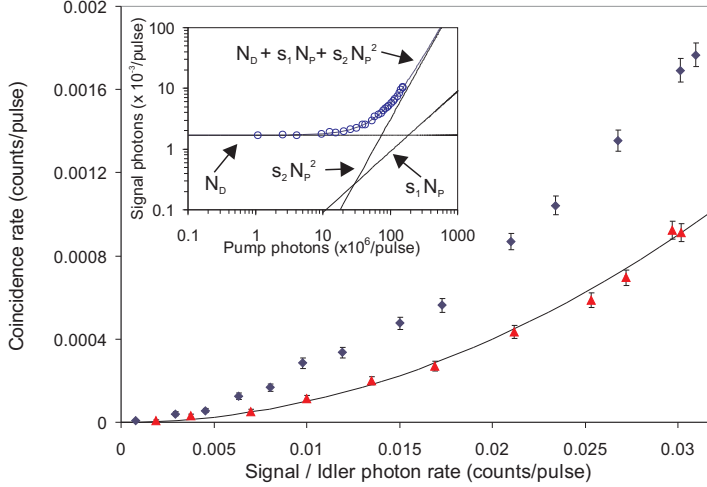


Figure 2. Coincidence rates as a function of the single-photon rates in two different cases: signal-idler fluorescence produced by a pump pulse (diamonds) and signal-idler fluorescence produced by two consecutive pump pulses (triangles). The line represents the calculated “accidental” counts. The inset shows a plot of the detected signal (or idler) photons as a function of the injected pump photons (hollow circles). A second-order polynomial is shown to fit the experimental data. The contributions of the dark counts, linear scattering, and quadratic scattering are plotted separately as well.

NFSI. We fit the experimental data with $N_I = N_D + s_1 N_P + s_2 N_P^2$, where N_D is the number of dark counts during the gate interval, and s_1 and s_2 are the linear and quadratic scattering coefficients, respectively. The fit clearly shows that the quadratic scattering owing to four-photon mixing in the fiber can dominate over the residual linear scattering of the pump due to imperfect filtering. The main body of Fig. 2 shows the coincidence counting results. The diamonds represent the rate of coincidence counts as a function of the geometric mean of the rates of the signal and idler photons generated during the same pump pulse. Dark counts have been subtracted from the plotted count rates. The triangles in Fig. 2 represent the measured coincidence rate as a function of the signal-photon count rate when the signal is delayed with respect to the idler by one pulse period. For two independent photon sources, each with a count rate $R_S \ll 1$, the “accidental” coincidence rate R_C is given by $R_C = R_S^2$, regardless of the photon statistics of the sources. This quadratic relation is plotted as the solid line in Fig. 2, which fits the delayed-coincidence data (triangles) very well. These measurements then show that while the fluorescence photons produced by the adjacent pump pulses are independent, those coming from the same pump pulse show a strong correlation, which is a signature of their nonclassical behavior.

With 75 MHz pump-pulse rate, we are now routinely detecting over 1500 photon pairs/s, which we expect to push up by a factor of 20 with further

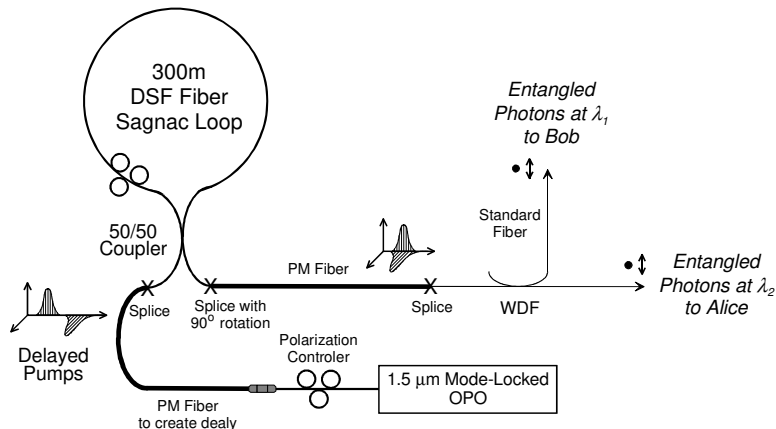


Figure 3. Schematic of an all-fiber experiment to create polarization-entangled photon pairs. In our current implementation, the relatively-delayed, orthogonally-polarized pumps at the input are created with bulk-optic components. The delay at the output, however, is removed by use of a polarization-maintaining (PM) fiber, as shown. Similarly, in our current setup the polarization-entangled photon pairs generated in the Sagnac loop are separated at the output with a bulk-optic wavelength-dependent filter (WDF). An approximately 400-m long all-fiber polarization interferometer is formed between the entrance surface of the input PM fiber and the exit surface (just before the WDF) of the output PM fiber.

refinements in the detection apparatus. Use of higher repetition rate pump pulses (over 10 GHz rate is possible with mode-locked fiber lasers) has the potential of increasing this rate by another two orders of magnitude. As we demonstrate in Sec. 3 below, polarization-entangled photon pairs can then be obtained by polarization multiplexing the signal and idler photons from two orthogonally-polarized pumps.

3 A Fiber-Optic Source of Polarization Entanglement

In this section we present the first, to the best of our knowledge, all-fiber source of polarization-entangled photon pairs. This source has the advantage of modal purity over its crystal counterparts,^{2,3} which is very important for realizing complex networks involving many quantum operations.

As demonstrated in Sec. 2 above, the parametric fluorescence accompanying nondegenerate four-wave mixing in standard optical fibers is an excellent source of quantum-correlated photon pairs.⁵ The quantum correlations arise because the parametric fluorescence is a result of two pump photons scattering through the Kerr nonlinearity to create simultaneous signal and idler photons. In order to create polarization-entangled photon pairs, we take advantage of the fact that the parametric fluorescence in standard fiber is predominantly co-polarized with the pump. When the Sagnac loop is pumped with two delayed orthogonally-polarized pulses, see Fig. 3, the down-converted signal and

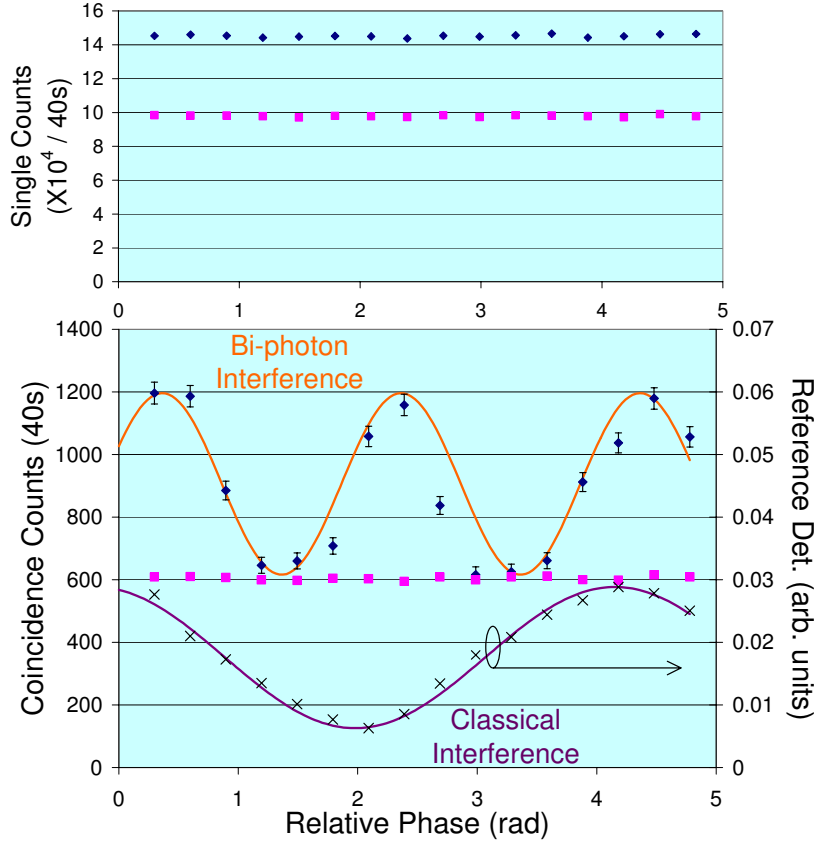


Figure 4. Top Plot: Single-photon counts registered by the signal (diamonds) and the idler (squares) detectors as the phase between the two pump pulses is varied. No phase dependence is observed in either detector's count rate. Bottom Plot: Coincidence-photon counts (diamonds) registered by the signal and idler detectors as the phase between the two pump pulses is varied. The squares represent accidental coincidences that are measured due to less-than-unity detection efficiency and dark counts in the detectors. After subtraction of the accidental counts, the resulting fringe visibility is $> 90\%$. The period of the fringes is half that of the classical interference fringes (crosses, right scale), which were simultaneously monitored by a reference detector during the coincidence measurements. The solid lines are best fits to the expected sinusoidal dependencies.

idler photons originating from the two pulses are co-polarized with the corresponding pumps. However, when the delay distinguishing the down-converted photons is removed and the signal/idler photons are wavelength separated, then a polarized single-photon detection event at the output, in either the signal or the idler arm, cannot determine which pump-pulse produced the photon. This indistinguishability results in polarization entanglement of the signal and idler photons, which we demonstrate by means of interference in coincidence-photon counting of the polarized signal and idler outputs. The

coincidence-rate should vary sinusoidally as the relative phase between the two pump pulses is scanned.

Similar nonclassical interference has previously been demonstrated by Ou *et al.* with use of two separate $\chi^{(2)}$ -crystal based spontaneous parametric down-converters.^{6,7} The observed visibility was 40%. The two-interferometer setup in their experiment was of the Mach-Zehnder type, whereas in our experiment the two-interferometer is formed by temporally multiplexing an all-fiber polarization interferometer. This interference effect is based on pairs of photons (biphotons) rather than single photons, which led Ou *et al.* to the remark: “Indeed it is possible to modify Dirac’s famous statement and argue that pairs of photons are interfering with themselves in these experiments.”⁷

A summary of the details of our observations is given in the caption of Fig. 4. We observe a visibility of $> 90\%$ in the interference fringes that occur in coincidence counting. Classically, no interference is expected in such coincidence counts.

Acknowledgments

This work was supported by the Department of Defense Multidisciplinary University Research Initiative (MURI) program administered by the Army Research Office under Grants DAAD19-00-1-0177 and DAAD19-00-1-0469, and by the U. S. Office of Naval Research under Grant N00014-91-J-1268.

References

1. C. H. Bennett and P. W. Shor, “Quantum Information Theory,” *IEEE Trans. Inf. Theory* **44**, 2724 (1998).
2. P. G. Kwiat, E. Waks, A. G. White, I. Appelbaum, and P. H. Eberhard, “Ultrabright source of polarization-entangled photons,” *Phys. Rev. A* **60**, R773 (1999).
3. S. Tanzilli, H. De Riedmatten, W. Tittel, H. Zbinden, P. Baldi, M. De Micheli, D. B. Ostrowsky and N. Gisin, “Highly efficient photon-pair source using periodically poled lithium niobate waveguide,” *Electron. Lett.* **37** 26 (2001).
4. J. E. Sharping, M. Fiorentino, and P. Kumar, “Observation of twin-beams type quantum correlation in optical fiber,” *Opt. Lett.* **26**, 367 (2001).
5. M. Fiorentino, P. L. Voss, J. E. Sharping, and P. Kumar, “All-fiber photon-pair source for quantum communications,” *Photon. Technol. Lett.* **14**, 983 (2002).
6. Z. Y. Ou, L. J. Wang, and L. Mandel, “Vacuum effects on interference in two-photon down conversion,” *Phys. Rev. A* **40**, 1428 (1989).
7. Z. Y. Ou, L. J. Wang, X. Y. Zou, and L. Mandel, “Evidence for phase memory in two-photon down conversion through entanglement with the vacuum,” *Phys. Rev. A* **41**, 566 (1990).